Hindawi
Journal of Spectroscopy
Volume 2017, Article ID 3290420, 7 pages
https://doi.org/10.1155/2017/3290420

Research Article

Study on the Noise Reduction of Vehicle Exhaust NO_X Spectra Based on Adaptive EEMD Algorithm

Kai Zhang,[1,2,3] Yujun Zhang,[1] Kun You,[1] Ying He,[1,2] Qiankun Gao,[1,2] Guohua Liu,[1,2] Chungui He,[1,2] Yibing Lu,[1,2] Boqiang Fan,[1,2] Qixing Tang,[1,2] and Wenqing Liu[1]

[1]*Key Laboratory of Environmental Optics and Technology, Anhui Institute of Optics and Fine Mechanics, Chinese Academy of Sciences, Hefei, Anhui Province 230031, China*
[2]*University of Science and Technology of China, Hefei, Anhui Province 230026, China*
[3]*Key Laboratory of Optical Monitoring Technology for Environment, Hefei, Anhui Province 230031, China*

Correspondence should be addressed to Kai Zhang; kaizhang@aiofm.ac.cn

Received 24 February 2017; Accepted 18 April 2017; Published 12 June 2017

Academic Editor: Artem E. Masunov

It becomes a key technology to measure the concentration of the vehicle exhaust components with the transmission spectra. But in the conventional methods for noise reduction and baseline correction, such as wavelet transform, derivative, interpolation, polynomial fitting, and so forth, the basic functions of these algorithms, the number of decomposition layers, and the way to reconstruct the signal have to be adjusted according to the characteristics of different components in the transmission spectra. The parameter settings of the algorithms above are not transcendental, so with them, it is difficult to achieve the best noise reduction effect for the vehicle exhaust spectra which are sharp and drastic in the waveform. In this paper, an adaptive ensemble empirical mode decomposition (EEMD) denoising model based on a special normalized index optimization is proposed and used in the spectral noise reduction of vehicle exhaust NO_X. It is shown with the experimental results that the method can effectively improve the accuracy of the spectral noise reduction and simplify the denoising process and its operation difficulty.

1. Introduction

With the increase of the motor vehicle quantity in China, the vehicle exhaust pollution becomes more and more serious. The continuous haze weather and exceeding of PM2.5 standard are all related to the vehicle emissions. So it is urgent to monitor and control the vehicle exhaust emissions [1]. At present, the method of using spectral information to retrieve the exhaust component concentration has become the mainstream technology for the vehicle exhaust detection, so it is very important to reduce noise of the vehicle exhaust transmission spectra.

The ultraviolet transmission spectra within 200–400 nm band are commonly used to analyze the concentration of the exhaust NO_X components. However, there are mainly three kinds of noises in the ultraviolet spectra, which are the electronic thermal noise, the light source fluctuation, and the interference of external communication systems. The location, amplitude, energy and width information, and so forth of NO_X spectral peaks are seriously affected by these noises. So it is necessary to denoise the NO_X ultraviolet transmission spectra in order to obtain clear and reliable spectral data, which is of great importance for the further analysis and concentration inversion. There are many absorption peaks of small amplitude and low energy in the exhaust NO_X spectra, of which the waveforms are sharp and drastic and their effective information frequency is high. When the traditional methods are used to reduce the spectral noise, the high frequency parts with the effective information often get lost, which result in the spectral peak shifting or its intensity changing. Therefore, it is necessary to study the noise reduction method suitable for the cross-mixed condition of the high frequency signal and noise.

2. Adaptive EEMD Denoising Algorithm

2.1. Normal EEMD Denoising Algorithm and Its Deficiency. Empirical mode decomposition (EMD) is a signal processing method proposed by Huang et al. in 1998 [2–4], with which one signal can be decomposed into a finite number of intrinsic mode functions (IMF). IMF can meet the global narrowband requirement and local zero-mean condition, but there exists mode mixing problems when it is used to decompose the signal [5, 6]. Therefore, the ensemble empirical mode decomposition (EEMD) method is proposed by Huang et al. [7], in which the Gauss white noise is added into the signal to be processed so as to provide enough extreme points for smoothing abnormal events, and then the IMF components obtained by multiple decompositions are overall averaged to overcome the mode mixing. At last, the Gauss white noise can be eliminated with the ensemble average process above.

There are two main steps in the EEMD decomposition. Step 1: Gauss white noises of equal length and random amplitudes are added into the signal to be processed, then the mixed signal is decomposed with EMD, after the above process is repeated K times; finally, the IMF component c_{ik} and the remainder r_{ik} are obtained. It is pointed out that the amplitude of white noises should follow the rule below:

$$a = ek \quad \text{or} \quad \ln e + 0.5a \ln k = 0, \tag{1}$$

where e is the standard deviation of the original signal, which is the deviation between the signal and the reconstruction result with EMD a is the white noise amplitude. It can be drawn that when the amplitude of the white noise increases, the repeat number K of EMD decomposition should be increased to reduce the effect of noise on the decomposition results. When the signal to be processed is mainly consisting of high frequency components, the amplitude a should be smaller and vice versa [8]. And the noise amplitude will not affect the decomposition results, unless it is very small or large. Therefore, the EEMD processing results will not change too much with the different settings of one or several parameters, which means the EEMD method is adaptive and does not rely on the subjective intervention of human beings.

Step 2: IMF components are overall averaged as the following:

$$\mathrm{IMF}_i = \frac{1}{n}\sum_{k=1}^{n} \mathrm{IMF}_{ik}, \qquad r_i = \frac{1}{n}\sum_{k=1}^{n} r_{ik}, \tag{2}$$

where n is the number of EMD decomposition. In this paper, the vehicle exhaust NO_X transmission spectra after EEMD decomposition have been reconstructed, and its error probability less than 10^{-9} is 99.2317%, which means that using EEMD to decompose the NO_X transmission spectra is approximately complete. In the process of EMD or EEMD decomposition in which there exists no mode mixing, each IMF has different frequency components and the IMFs of high frequency are always the first to be screened. So the decomposition process is considered as multiple band-pass filtering, and then by constructing a low-pass filter, the noise reduction can be realized [6–8].

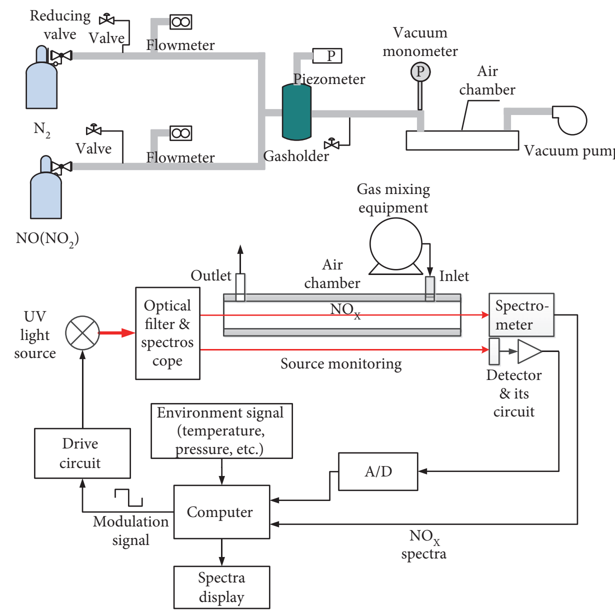

Figure 1: Schematic diagram of the experimental platform with its gas mixing equipment for NO_X spectra acquisition.

In the construction process of EMD or EEMD low-pass filter, the order of the reconstructed signal is an important parameter of the filter and the selection of which is crucial to the denoising accuracy. Usually, a posterior denoising performance index is used to determine the parameters, which requires the index to evaluate the denoising effect from respects of the spectral deformation degree and SNR, and so forth. However, when the signal and noise exist in the same IMF component simultaneously, it will be all reserved or filtered by the low-pass filter in EMD or EEMD process, which will lead to low noise reduction accuracy [9, 10]. In order to solve the problem mentioned above, a normalized evaluation index is designed in the paper, with which the method of cyclic decomposition and reconstruction is used to improve denoising accuracy of EEMD.

2.2. Design of the Normalized Optimization Index for EEMD Denoising. A new EEMD method based on a special normalized index optimization is proposed here, of which the global optimum of the normalized denoising index is used as the stopping condition of the reduction process, so the process does not need any parameter setting and can be completed automatically. The signal to noise ratio (SNR), standard error (SE), and correlation coefficient (R) are used for the index to evaluate the noise reduction effect. In order to express the comprehensive change of energy, shape, and position of the spectra after the noise reduction, the normalized index r is designed as follows:

$$r = \left| \frac{\mathrm{SNR}' - \mathrm{SNR}}{\mathrm{SNR}} + \frac{1}{\mathrm{SE}} + R \right|, \tag{3}$$

(a) Photo of the experimental system with 100 cm gas chamber

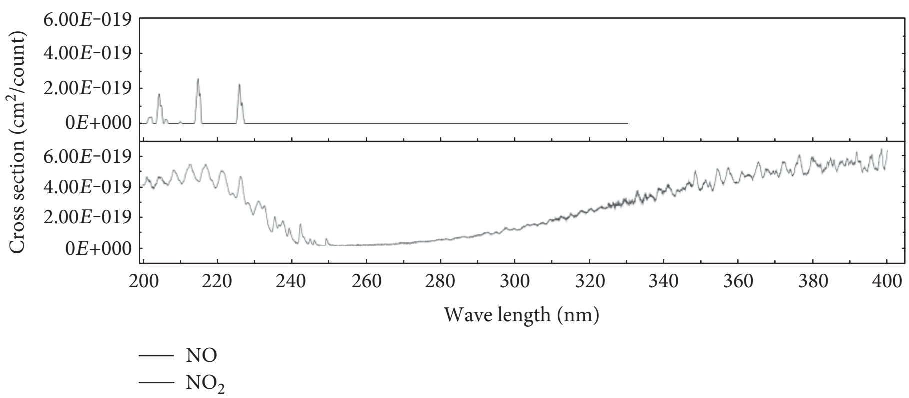

(b) Absorption cross-sections of NO and NO_2 in the near UV band

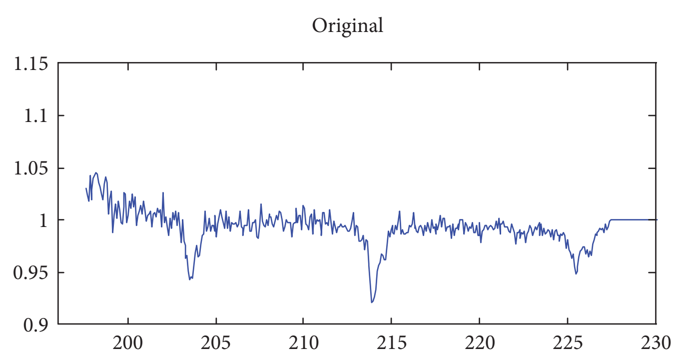

(c) NO-40 cm-16 ppm

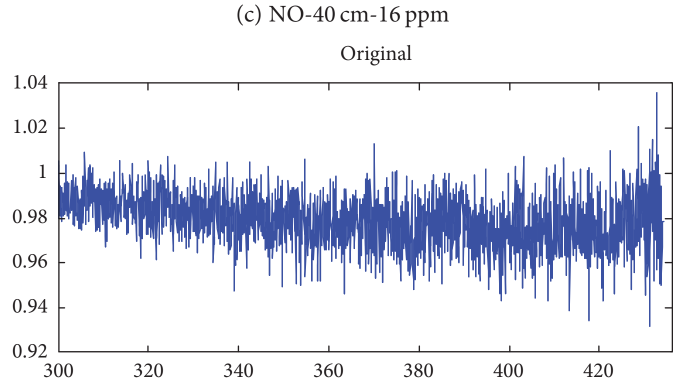

(d) NO_2-100 cm-25 ppm

Figure 2: Transmission spectra of NO and NO_2 at lower concentrations.

where SNR$'$ stands for the signal to noise ratio after the spectral noise reduction. The index r combines two aspects of spectral details and approximation information to evaluate the effect of noise reduction, and it can make sure that the indexes of the two aspects are negatively correlated, so the greater the value of r, the better [9].

3. Denoising Experiment and Analysis

3.1. Acquisition of NO_X Transmission Spectra from the Vehicle Exhaust. As shown in Figure 1, the experimental platform with a gas mixing equipment for acquisition of NO_X transmission spectra from the vehicle exhaust has been built, with its photo being shown in Figure 2(a). UV absorption cross-sections of NO and NO_2 are shown in Figure 2(b). Then NO and NO_2 UV transmission spectra (200 nm–440 nm) of different concentrations and absorption path have been obtained with the platform, also with their mixture transmission spectra. The transmission spectra of 16 ppm NO is shown in Figure 2(c), and the spectra of 25 ppm NO_2 is shown in Figure 2(d).

With the obtained spectra, it can be drawn that the noise is obvious and it affects SNR seriously in the lower concentration measurement, which will be the accurate concentration inversion of NO and NO_2 gas. So it is necessary to carry on the noise reduction before the concentration inversion.

3.2. Denoising Experiment Based on EEMD and Data Analysis. The noise reduction algorithm is designed with EEMD method being combined with the normalized index r, of which the denoising flow chart is shown in Figure 3.

Step 1: the spectral signal x_i is decomposed with EEMD, and then n IMF components have been obtained (there is no special operation for the residual during denoising process, and the residual is recorded as IMF_n).

Step 2: the low order component IMF_1 with high frequency is removed, and then the spectral signals are reconstructed to form a new spectrum, which is recorded as x_{i+1}.

Step 3: to calculate the indeces r_{i+1}, x_i, and x_{i+1} are put into the following formulas:

$$\mathrm{SNR} = 10\log\frac{S}{N} = 10\log\left(\frac{\sum_{j=1}^{n} x_{i+1}^{2}(j)}{\sum_{j=1}^{n}\left[x_i(j) - x_{i+1}(j)\right]^2}\right),$$

$$\mathrm{SE} = \sqrt{\frac{1}{n}\sum_{j=1}^{n}\left[x_i(j) - x_{i+1}(j)\right]^2}, \qquad (4)$$

$$R = \frac{\sum_{j=1}^{n}\left(x_i(j) - \overline{x_i}\right)\left(x_{i+1}(j) - \overline{x_{i+1}}\right)}{\sqrt{\sum_{j=1}^{n}\left(x_i(j) - \overline{x_i}\right)^2}\sqrt{\sum_{j=1}^{n}\left(x_{i+1}(j) - \overline{x_{i+1}}\right)^2}},$$

where $\overline{x_i} = \frac{1}{n}\sum_{j=1}^{n} x_i(j)$, $\overline{x_{i+1}} = \frac{1}{n}\sum_{j=1}^{n} x_{i+1}(j)$, n is the amount of data in each spectrum. And then, SNR, SE, and R can be put into (4) to calculate the index r_{i+1}.

Step 4: after the index r_{i+1} is calculated, if $r_{i+1} > r_i$, it means that the normalized index has been optimized

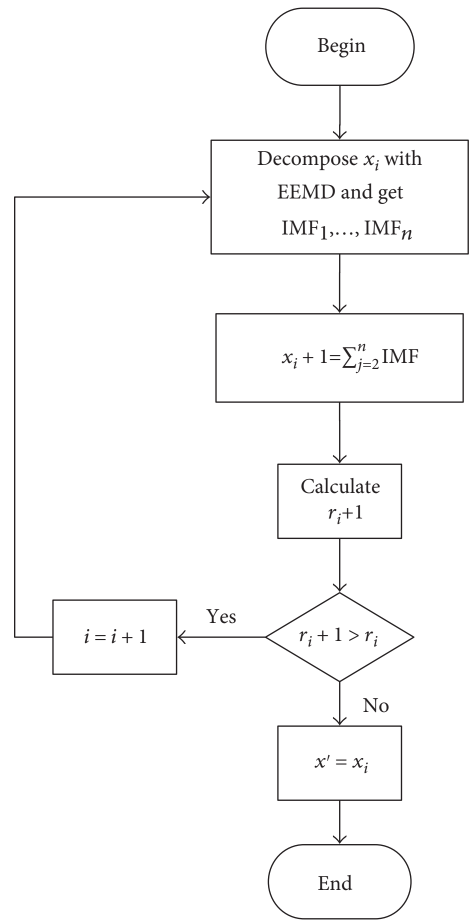

Figure 3: Adaptive EEMD denoising flow chart based on normalized index optimization.

with the $(i+1)$th denoising, so there is a possibility of decomposition, filtering, and reconstruction for the spectral signals once more; then, $i = i + 1$ is set and the whole denoising procedure returns to step 1. If $r_{i+1} < r_i$, it means that the best EEMD optimal normalized index has been obtained with the ith denoising, the EEMD noise reduction process ends, and x_i is the best result with NIO EEMD denoising, at last the signal x_i is assigned to x' ($x' = x_i$).

According to the algorithm and flow chart above, the EEMD Matlab procedure has been programmed, and then it is used for denoising of three NO_X UV transmission spectra. The results are shown in Figure 4. SNR of the three spectra before and after denoising is compared in Table 1, and the NO_X absorbance and inverted concentrations at their respective peaks are listed in Table 2. It can be drawn from the experimental results in the two tables that SNR of the transmission spectra have been improved after denoising, and the absorbance and inverted concentrations are closer to the theoretical value calculated with the experimental system parameters.

Then EMD low-pass filter [5, 6], db3 wavelet decomposition [10], and NIO EEMD are used, respectively, for noise reduction of one NO_X mixed transmission spectrum (NO_2-300 ppm/NO-786 ppm/100 cm) to further verify the

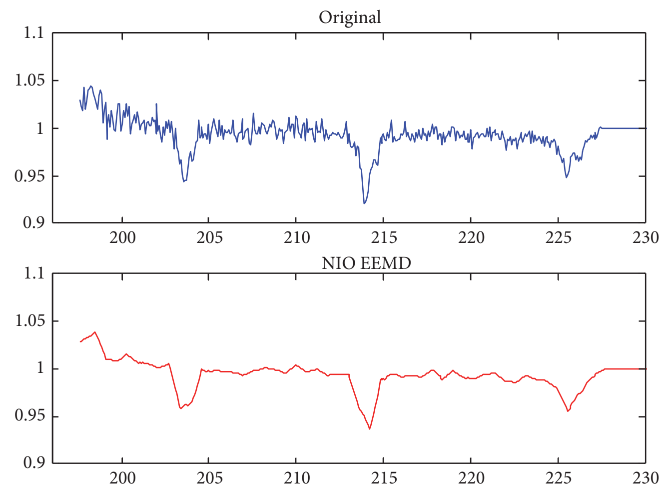

(a) NO_2-100 cm-25 ppm

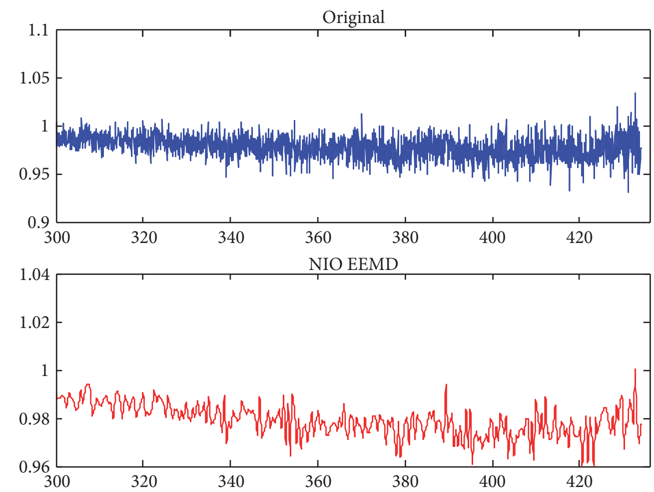

(b) NO_2-100 cm-25 ppm

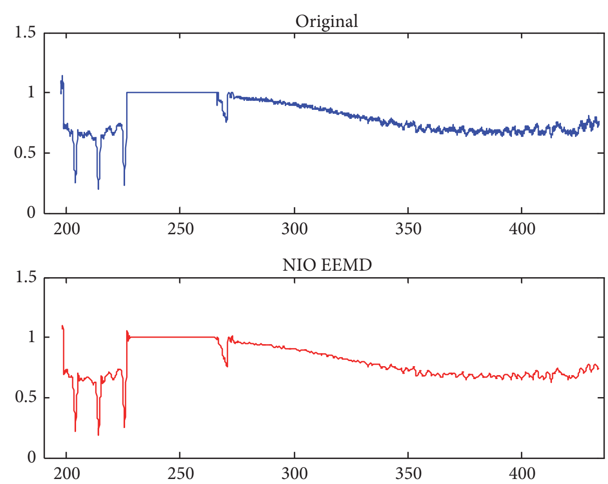

(c) NO_2-300 ppm-NO-786 ppm-100 cm

Figure 4: Three NO_X spectra before and after denoising with NIO EEMD.

Table 1: SNR of NO_X spectra of different concentrations before and after denoising.

Gas	Absorption length	Sample gas concentration	SNR/dB	SNR′/dB
NO	40 cm	16 ppm	17.5626	25.5619
NO	40 cm	1572 ppm	19.1573	24.3398
NO	100 cm	16 ppm	18.2774	26.1679
NO	100 cm	1310 ppm	19.1125	26.0135
NO_2	40 cm	25 ppm	16.3378	25.7757
NO_2	40 cm	500 ppm	18.9986	25.3589
NO_2	100 cm	25 ppm	18.4318	24.4095
NO_2	100 cm	300 ppm	19.8761	27.0057
NO_2/NO	100 cm	100/1310 ppm	23.0499	28.9197
NO_2/NO	100 cm	200/1048 ppm	22.8761	28.1918
NO_2/NO	100 cm	300/786 ppm	22.0731	28.1347
NO_2/NO	100 cm	500/262 ppm	21.7682	27.6987

denoising effect of NIO EEMD method. As shown in Figure 5(b), EMD low-pass filtering method has been used for one decomposition, and then the first order IMF component has been removed, finally there still exists a lot of noise in the denoised spectrum, and the three NO absorption peaks in 200–230 nm band have a large deformation. The reason is that the EMD decomposition produces a mode mixing which has been filtered with the useful signals from the original spectrum. As shown in Figure 5(c), db3 wavelet basis with 5-layer decompositions and soft threshold method has been used to construct the wavelet model for filtering and denoising, finally a certain amount of noise is still left in the spectrum. At last, the noise reduction effect of adaptive NIO EEMD method is shown in Figure 5(d).

Denoising indexes of the three algorithms are shown in Table 3, where LPF stands for the low-pass filter and NIO indicates that the noise reduction method bases on normalized index optimization mentioned above. There are absorbance values and inverted concentrations of the same spectral with three denoising algorithms listed in Table 4.

Table 2: Absorbance and inverted concentrations of NO_X before and after noise reduction.

Gas	Absorption wavelength & length	Sample gas concentration	Theoretical absorbance	Absorbance before denoising	Concentration before denoising	Absorbance after denoising	Concentration after denoising
NO	215.3 nm-40 cm	16 ppm	0.0269	0.0356	21.17 ppm	0.0221	13.15 ppm
NO	215.3 nm-40 cm	1572 ppm	2.6429	2.6587	1581.4 ppm	2.6407	1570.7 ppm
NO	215.3 nm-100 cm	16 ppm	0.0673	0.0798	18.76 ppm	0.0691	16.43 ppm
NO	215.3 nm-100 cm	1310 ppm	5.5102	5.5363	1318.2 ppm	5.5099	1309.9 ppm
NO_2	430.7 nm-40 cm	25 ppm	0.0031	0.0123	99.01 ppm	0.0057	45.97 ppm
NO_2	430.7 nm-40 cm	500 ppm	0.0616	0.0805	653.4 ppm	0.0569	461.9 ppm
NO_2	430.7 nm-100 cm	25 ppm	0.0077	0.0136	44.16 ppm	0.0085	27.59 ppm
NO_2	430.7 nm-100 cm	300 ppm	0.0924	0.1243	400.6 ppm	0.0956	310.4 ppm
NO_2/NO	226.5 nm-100 cm	100/ 1310 ppm	0.9841	0.9997	101.6/ 1330.8 ppm	0.9912	100.7/ 1319.4 ppm
NO_2/NO	226.5 nm-100 cm	200/ 1048 ppm	0.8243	0.8339	202.4/ 1060.2 ppm	0.8217	199.4/ 1044.7 ppm
NO_2/NO	226.5 nm-100 cm	300/786 ppm	0.6028	0.6329	314.9/825.5 ppm	0.5988	298/780.8 ppm
NO_2/NO	226.5 nm-100 cm	500/262 ppm	0.3446	0.3621	525.4/275.4 ppm	0.3399	493.2/259.4 ppm

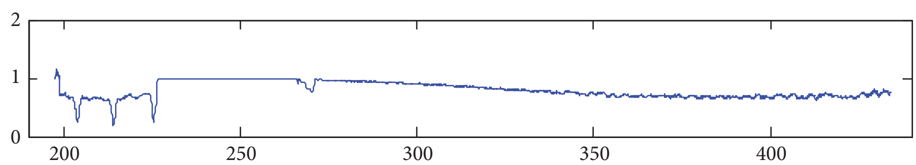

(a) Original

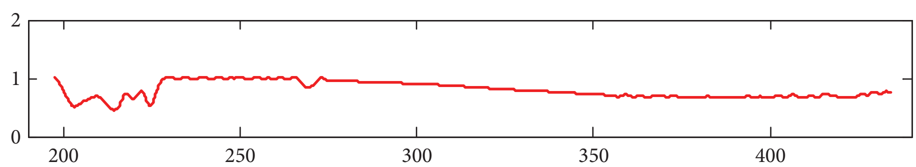

(b) EMD LPF

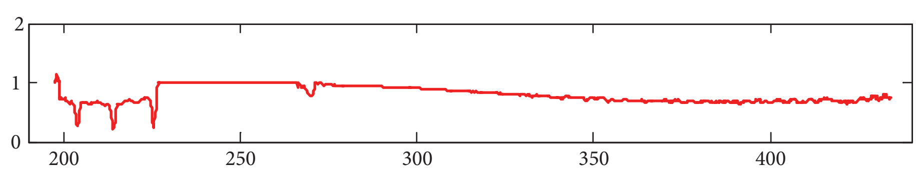

(c) Wavelet

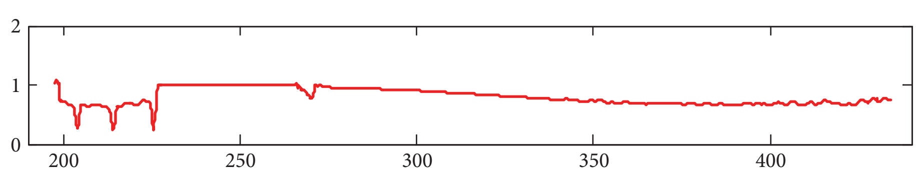

(d) EEMD NIO

Figure 5: Comparison of denoising effect among adaptive NIO (normalized index optimization) EEMD and other algorithms.

Table 3: Denoising indexes of the three algorithms.

	SNR′/dB	SE	R	r
EMD LPF	21.1201	0.8017	0.9624	2.2094
Wavelet	22.8221	0.8023	0.9975	2.2236
NIO EEMD	28.1347	0.8025	0.9994	2.2455

Table 4: Absorbance and inverted concentrations before and after noise reduction with three algorithms.

NO_2/NO:300/786 ppm, $\lambda = 226.5$ nm, $L = 100$ cm	Theoretical absorbance	Before noise reduction	Concentration before denoising	After noise reduction	Concentration after denoising
EMD LPF				0.3360	169.3/439.2 ppm
Wavelet	0.6028	0.6329	314.9/825.5 ppm	0.5782	287.8/753.9 ppm
NIO EEMD				0.5988	298.3/780.8 ppm

Compared with the original spectrum data, better denoising effect can be obtained adaptively with NIO EEMD method, due to which the calculation accuracy of the absorbance can be improved also with the retrieval precision of NO_X gas concentrations. Meanwhile, the other two algorithms have strong dependence on parameter settings, and once the parameters are not set properly, the denoising effect will be affected obviously.

4. Conclusion

In this paper, the EEMD method is used to decompose the UV transmission spectra of NO_X from vehicle exhaust; then, a normalized noise performance index has been constructed, according to the global extremum of which the cycle order of the EEMD decomposition on the transmission spectra can be determined adaptively. The parameters such as basis function, threshold value, and decomposition layer do not have to be set with this method, so that the noise reduction effect of NO_X spectrum does not rely on whether the setting of parameters is appropriate. With the experimental results, it can be concluded that when using in the denoising of the NO_X transmission spectra, the EEMD algorithm based on normalized index optimization is better than the EMD low-pass filter and the db3 wavelet decomposition algorithm in the same situation.

Conflicts of Interest

The authors declare that there are no conflicts of interest.

Acknowledgments

The work is supported by the National Key Research and Development Program of China (2016YFC0201003) and the 863 National High Technology Research and Development Program of China (no. 2014AA06A503).

References

[1] C. Ping, "The present situation of urban air pollution in China and its integrated control strategy," *Environmental Science and Management*, vol. 31, no. 1, pp. 18–21, 2006.

[2] N. E. Huang, S. Zheng, S. R. Long et al., "The empirical mode decomposition and the Hilbert spectra for nonlinear and non-stationary time series analysis[J]," *Proceedings of the Royal Society of London A*, vol. 454, no. 1971, pp. 903–995, 1998.

[3] A. Verma, Pratik, and G. Pradhan, "Electrocardiogram denoising using wavelet decomposition and EMD domain filtering," in *2016 IEEE Region 10 Conference (TENCON)*, pp. 2185–2189, Singapore, Singapore, November 2016.

[4] A. G. Mahapatra and K. Horio, "Overcoming drawback of feature instantaneous bandwidth using EMD for epileptic seizure classification by RMS frequency," in *2016 IEEE International Conference on Systems, Man, and Cybernetics (SMC)*, pp. 001322–001327, Budapest, Hungary, October 2016.

[5] J. Singh, A. K. Darpe, and S. P. Singh, "Bearing damage assessment using Jensen-Renyi Divergence based on EEMD[J]," *Mechanical Systems and Signal Processing A*, vol. 87, pp. 307–339, 2017.

[6] T. Goetz, L. Stadler, G. Fraunhofer, A. M. Tomé, H. Hausner, and E. W. Lang, "A combined cICA-EEMD analysis of EEG recordings from depressed or schizophrenic patients during olfactory stimulation," *Journal of Neural Engineering*, vol. 14, no. 1, p. 016011, 2016.

[7] W. Wang and X. Chen, "The temperature compensation method of fiber optic gyroscope based on EEMD, B-Spline and SVM," in *2016 IEEE Chinese Guidance, Navigation and Control Conference (CGNCC)*, pp. 512–516, Nanjing, China, August 2016.

[8] K. Deng, D. Jian-li, A. X. Yang, and Z. Y. Niu, "EEMD denoising of reflecting spectrum in soil profiles," *Spectroscopy and Spectral Analysis*, vol. 35, no. 1, pp. 162–166, 2015.

[9] X. Zhao, *Research and Application on Adaptive Spectra Preprocessing Methods Based on EMD and EEMD [D]*, pp. 22–23, Yanshan University, Yanshan, Hebei, China, 2015.

[10] S. Zhang, Y. Shi, S. Gao et al., "Analysis method of microstructure surface topography based on wavelet filter," in *International Conference on Optoelectronics and Microelectronics Technology and Application, Proc. SPIE*, Shanghai, China, January 05, 2017.